SCIENTIFIC REPORTS

OPEN

Beam wander relieved orbital angular momentum communication in turbulent atmosphere using Bessel beams

Yangsheng Yuan[1,2,*], Ting Lei[1,*], Zhaohui Li[3], Yangjin Li[4], Shecheng Gao[1], Zhenwei Xie[1] & Xiaocong Yuan[1]

Optical beam wander is one of the most important issues for free-space optical (FSO) communication. We theoretically derive a beam wander model for Bessel beams propagating in turbulent atmosphere. The calculated beam wander of high order Bessel beams with different turbulence strengths are consistent with experimental measurements. Both theoretical and experimental results reveal that high order Bessel beams are less influenced by the turbulent atmosphere. We also demonstrate the Bessel beams based orbital angular momentum (OAM) multiplexing/demultiplexing in FSO communication with atmospheric turbulence. Under the same atmospheric turbulence condition, the bit error rates of transmitted signals carried by high order Bessel beams show smaller values and fluctuations, which indicates that the high order Bessel beams have an advantage of mitigating the beam wander in OAM multiplexing FSO communication.

Optical multiplexing has dramatically increased capacity and spectral efficiency in free space optical (FSO) communication and fiber optical communication. Multiplexing technologies have been proposed and demonstrated including spatial-division multiplexing[1], polarization-division multiplexing[2], frequency-division multiplexing[3], wavelength-division multiplexing[4] and mode-division multiplexing (MDM)[5,6]. Orbital angular momentum (OAM) multiplexing as a special case of MDM has been considered as a good candidate for high capacity optical communication. An optical beam carrying OAM, namely optical vortex (OV) beam, is associated with the helical shaped wavefront and the donut shaped intensity distribution. The phase term of $\exp(in\varphi)$ describes the helical transverse mode, where n is an integer indicating the topological charge of photons with $n\hbar$ orbital angular momentum and φ is the azimuthal angle[7]. The OAM beams have widely been studied for particle trapping[8], image processing[9], astronomy[10] and photon sorting[11]. The OAM beams with mutually orthogonal property have also been implemented for multiplexing/demultiplexing in FSO communication[5,6].

In FSO communication, major challenges come from the atmospheric turbulence induced optical phase wavefront aberrations, intensity fluctuations and beam wanders[12–16]. The power fluctuations and mode crosstalk in optical communication system have been investigated theoretically and experimentally[17–22]. For OAM communication, the atmospheric turbulence influences for OAM states crosstalk have theoretically been studied in single-photon and multichannel communication system[18,19]. OAM multiplexing based outdoor light communication with the propagation distance ranging from 120 m to 3 km have also been demonstrated recently[20–22]. The high order Bessel beam with a field of $J_n(k_r r) \exp(in\varphi)$ can also be considered as a beam carrying a OAM state of $\exp(in\varphi)$, where J_n is the Bessel function of order n, k_r is the radial wave vector components, and (r, φ) are the polar coordinates[13,23]. The propagations of the Bessel beam and Laguerre Gaussian beam through turbulent atmosphere are comparably studied in ref. 24. The investigation results show, in the same condition, the variance

[1]Nanophotonics Research Centre, Shenzhen University & key Laboratory of Optoelectronic Devices and Systems of Ministry of Education and Guangdong Province, College of Optoelectronic Engineering, Shenzhen University, Shenzhen, 518060, China. [2]Department of Physics, Anhui Normal University, Wuhu, 241000, China. [3]State Key Laboratory of Optoelectronic Materials and Technologies and School of Electronics and Information Technology, Sun Yat-sen University, Guangzhou, 510275, China. [4]Institute of Photonics Technology, Jinan University, Guangzhou, 510632, China. *These authors contributed equally to this work. Correspondence and requests for materials should be addressed to Z.L. (email: li_zhaohui@hotmail.com) or X.Y. (email: xcyuan@szu.edu.cn)
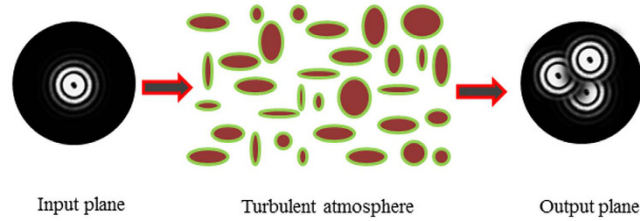
Figure 1. Schematic of the beam wanders for Bessel beam. Single Bessel beam in the input plane propagates through turbulent atmosphere. At the output plane, beam wanders are indicated by movements of the Bessel beam.

of fluctuations of the Bessel beam are smaller than that of the Laguerre Gaussian beam with the same topological charge. Compared with the conventional OAM beams, the Bessel beams show advantages in non-diffraction and self-healing, which can benefit the beam propagation in turbulent atmosphere[24–26]. For the coherent and partially coherent Bessel beams propagating through turbulent atmosphere, the statistical properties such as variance of fluctuations of the OAM[24], M^2–factor[25] and the variance of the displacement[26] are theoretical studied. The results show the Bessel-Gaussian beams are less affected by the turbulent atmosphere with larger values of topological charges[24–26]. However, the ref. 26 provides only the numerical calculations rather than analytical derivations to predict the trends of the variance of the displacement. The Bessel beams with non-diffraction and self-healing properties have been used in optical and millimeter-wave communication[27] and optical interconnect[28,29]. Therefore, the Bessel beams have the extraordinary properties may improve the OAM multiplexing based optical communications performances in turbulent atmosphere.

In this Letter, we investigate the high order Bessel beams based FSO communication with the turbulent atmosphere. Firstly, we derive an analytical formula for the beam wander of Bessel beams through turbulent atmosphere depending on the topological charge and turbulence strength. We also experimentally measure the beam wander of the Bessel beams with various topological charges. The results show that the Bessel beams with larger topological charges have smaller beam wander. Secondly, we build up a FSO communication system and characterize the Bessel beams based multiplexing technology in atmospheric turbulence. The measured BERs of the Bessel beams carrying the 10-Gbit/s on-off keying (OOK) signals can reach the forward error correction threshold.

Results

Principle and equations. Figure 1 schematically shows the beam wander of Bessel beams propagating through turbulent atmosphere, corresponding to the movements of the instantaneous beam center at the output plane. Turbulent atmosphere induces the crosstalk among different OAM states. In the following sections, we will accomplish the theoretical model of beam wander for Bessel beam in turbulent atmosphere, experimentally characterize the beam wander of high order Bessel beams at two temperatures different from room temperature and demonstrate the FSO communication using multiple coaxial Bessel beams propagating in turbulent atmosphere.

The Bessel beams with infinite power do not exist in reality. The Bessel Gaussian beams (BGBs) can be considered as approximate Bessel beams in experiments. When the Gaussian beam incident on the holograph with phase function of $\exp(-i2\pi r/r_0 + in\varphi)$, the nth order BGB can be generated[30,31]. The electric field of the nth order Bessel Gaussian beams is expressed as[25]

$$E_{BGB}(r, \varphi) = J_n\left(\frac{Rr}{w_0^2}\right)\exp\left(-\frac{r^2}{w_0^2}\right)\exp(in\varphi)$$

(1)

Here $R = 2\pi w_0^2/r_0$, w_0 is the waist width of the Gaussian beam.

Beam wander of the light propagating through the atmospheric turbulence can be described statistically by the variances of the displacements of the instantaneous beam center. The analytical expression of the beam wander available for weak, moderate and strong turbulence conditions is shown as[13]

$$\langle r_c^2 \rangle = 4\pi k^2 W_{FS}^2 \int_0^L \int_0^\infty \kappa \Phi_n(\kappa)\exp(-\kappa^2 W_{LT}^2)\left\{1 - \exp\left[-\frac{2L^2\kappa^2(1 - z/L)^2}{\kappa^2 W_{FS}^2}\right]\right\}d\kappa dz$$

(2)

Here κ is the spatial frequency, $k = 2\pi/\lambda$ is the wave number, λ is the wavelength, L is the propagation distance, and z is the distance of an intercept point on the propagation path. W_{LT} and W_{FS} are the long-term spot size with and without turbulence, respectively. $\Phi_n(\kappa)$ is the spatial power spectrum of the refractive-index fluctuations.

We can use the geometrical optics approximation in Eq. (2) and simplify the last term as[13]

$$1 - \exp\left[-\frac{2L^2\kappa^2(1 - z/L)^2}{\kappa^2 W_{FS}^2}\right] \cong \frac{2L^2\kappa^2(1 - z/L)^2}{\kappa^2 W_{FS}^2} \qquad L\kappa^2/k \ll 1$$

(3)

The Tatarskii spectrum is chosen as

$$\Phi_n(\kappa) = 0.033 C_n^2 \kappa^{-11/3} \exp(-\kappa^2/\kappa_m^2)$$

(4)

Here C_n^2 is the structure constant of the turbulent atmosphere, $\kappa_m = 5.92/l_0$ with l_0 as the inner scale.

By substituting Eqs (3) and (4) into Eq. (2), we obtain

$$\langle r_c^2 \rangle = 7.25 L^2 C_n^2 \int_0^L (1 - z/L)^2 (1/\kappa_m^2 + W_{LT}^2(z))^{-1/6} \, dz \tag{5}$$

According to the result obtained in ref. 13, W_{LT} can be expressed as the mean squared beam width $\langle W_{LT}^2 \rangle = \langle r_z^2 \rangle$.

Based on the second-order moments of the beam related to BGBs[25], we obtain the long-term beam width of the BGBs propagating through atmospheric turbulence

$$\langle W_{LT}^2 \rangle = \frac{w_0^2}{2} + \frac{2z^2}{k^2 w_0^2} \left[1 + \gamma + n + \frac{\gamma I_{n+1}(\gamma)}{I_n(\gamma)} \right] + \frac{w_0^2}{2} \left[n + \frac{\gamma I_{n+1}(\gamma)}{I_n(\gamma)} - \gamma \right] + \frac{4\pi^2 z^3}{3} Q \tag{6}$$

Here $\gamma = \pi^2 w_0^2 / r_0^2$, $I_n(\cdot)$ is the nth-order modified Bessel functions of the first kind, and $Q = \int \kappa^3 \Phi_n(\kappa) d\kappa$.

By substituting Eqs (4) and (6) into Eq. (5), the beam wander of the high order BGBs through turbulent atmosphere is obtained as Eq. (7).

$$\begin{aligned}
\langle r_c^2 \rangle = {} & 7.25 L^2 C_n^2 \int_0^L \left(1 - \frac{z}{L} \right)^2 \left[\frac{1}{\kappa_m^2} + \frac{w_0^2}{2} + \frac{2z^2}{k^2 w_0^2} \left(1 + \gamma + n + \frac{\gamma I_{n+1}(\gamma)}{I_n(\gamma)} \right) \right. \\
& \left. + \frac{w_0^2}{2} \left(n + \frac{\gamma I_{n+1}(\gamma)}{I_n(\gamma)} - \gamma \right) + \frac{0.6644 \pi^2 z^3}{3} C_n^2 l_0^{-\frac{1}{3}} \right]^{-1/6} dz
\end{aligned} \tag{7}$$

According to Eq. (5), the beam wander of Bessel Gaussian beams depends on the mean squared beam width. As shown in Eq. (6), there are larger mean squared beam widths with larger topological charges. From Eq. (7), the beam wander of the Bessel Gaussian beams propagation through turbulent atmosphere decreases with the increase of the topological charge.

Experiment and results. Figure 2(a) shows the experimental setup for Bessel beams based FSO communication in turbulent atmosphere. A continuous wave laser (CW Laser-1) at 1550 nm wavelength is fed into an optical modulator (Mod. −1) to produce the 10-Gbit/s OOK signals.

The signal laser is amplified by the high power erbium-doped fiber amplifier (EDFA), and then sent to the collimator (Col.) after the polarization controller (PC). In one branch, the collimated Gaussian beam with 4.65 mm diameter is projected onto reflective spatial light modulator (SLM-1) loaded with a special phase mask to generate the four collinear Bessel beams (Fig. 2b1). In the other branch, the collimated Gaussian beam is sent to the reflective SLM-2 loaded with another special phase mask to generate three coaxial superposition Bessel beams (Fig. 2c1). The combined multiplexed Bessel beams (Fig. 2d1) propagate through the turbulent atmosphere. The effects of atmospheric turbulence are simulated by the hot plate with controllable temperature. After propagating in turbulent atmosphere for 1.5 m, the collinear beams are sent to the reflective SLM-3 loaded with the optical vortex Dammann axicon grating.

The multiple high order Bessel beams generation with the Dammann grating have been demonstrated[32,33]. In this letter, the 1×7 optical vortex Dammann axicon grating is designed to detect the OAM states of the Bessel beams with topological charges of -6, -4, -2, 0, 2, 4 and 6. The grating parameters are chosen as follows: period $d = 0.12$ mm, topological charge interval $q = 2$ and the Bessel beam radius parameter $r_0 = 0.4$ mm.

The demultiplexed beams focusing with the lens (focal length is 60 mm) are captured by the infrared camera or coupled into single mode fiber (SMF) for direct detection. Figure 2(b1–d2) shows the images of multiplex/demultiplex Bessel beams. Figure 2(b1) shows the superimposed Bessel beams of J_{-6}, J_{-2}, J_2 and J_6 generated by SLM-1, which are demultiplexed by the grating loaded on SLM-3 (Fig. 2(b2)). Figure 2(c1) shows the superimposed Bessel beams of J_{-4}, J_0 and J_4 generated by SLM-2, which are demultiplexed by the grating loaded on SLM-3 (Fig. 2(c2)). Figure 2(d1) shows the superimposed Bessel beams of J_{-6}, J_{-4}, J_{-2}, J_0, J_2, J_4 and J_6 combined by the beam splitter, which are demultiplexed by the grating loaded on SLM-3 (Fig. 2(d2)). The collected signal beams from the SMF is amplified by the low power EDFA. The signal is monitored by the optical spectrum analyzer (OSA). The received demultiplexed Bessel beams carrying signals input into the oscilloscope for the bit-error-rate (BER) measurement under various optical signal-to-noise ratios (SNRs) adjusted by the tunable power attenuator.

Figure 3 shows central positions of high order Bessel beams (J_2, J_4 and J_{-6}) in turbulent atmosphere at the receive plane at 1.5 m away. For each figure, the superimposed dots are the centers of the Bessel beams recorded by the IR camera in 30 seconds with 448 frames.

The atmospheric turbulence is emulated by the hot plate and the turbulence strength is controlled by temperature difference δT[16]. The temperature gradient will generate convection air flow induced vertical turbulent atmosphere. In order to avoid air vortices, some iron needles are placed on the hot plate to form the inhomogeneous underlying surface. The beam wander can be extracted according to the displacements of the beams propagating through turbulent atmosphere. The structure constant C_n^2 can be calculated by the standard deviation of the displacement[13,20]. As shown in Fig. 3, the displacements of the Bessel beams increase with the temperature difference increasing for the same topological charge value. The displacements of the Bessel beams increase with the topological charge decreasing, for a fixed temperature difference.

As shown in Fig. 4, the beam wanders of the Bessel beam from the theoretical calculations and experimental results show the same trend. The beam wanders are obtained from mass derivations of the Bessel beam
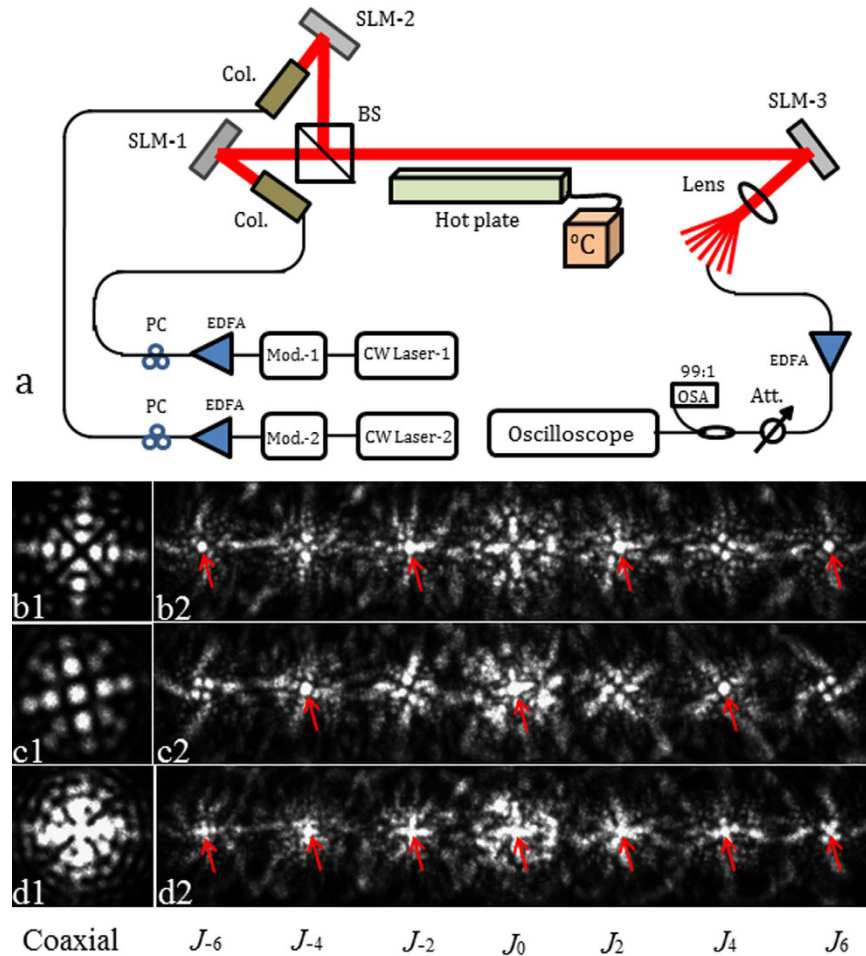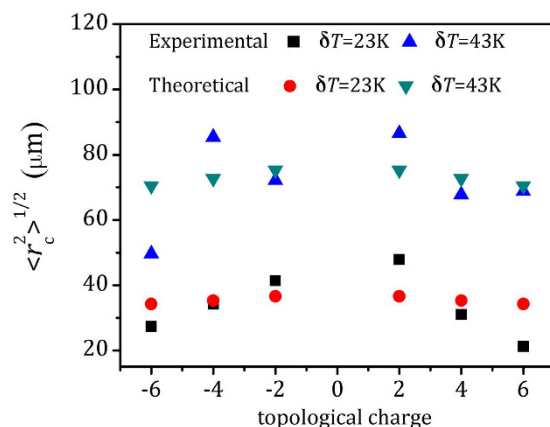
Figure 2. (**a**) Experimental setup of the Bessel beams through turbulent atmosphere in FSO communication system. (b1-d2) Images of the multiplexed/demultiplexed Bessel beams. (b1) the coaxial superposition Bessel beams with J_{-6}, J_{-2}, J_2 and J_6. (b2) the superposition Bessel beams (J_{-6}, J_{-2}, J_2 and J_6) demultiplexing simultaneously. (c1) The coaxial superposition Bessel beams with J_{-4}, J_0 and J_4. (c2) the superposition Bessel beams (J_{-4}, J_0 and J_4) demultiplexing simultaneously. (d1) the coaxial superposition Bessel beams with J_{-6}, J_{-4}, J_{-2}, J_0, J_2, J_4 and J_6. (d2) The combined multiplexed beams (J_{-6}, J_{-4}, J_{-2}, J_0, J_2, J_4 and J_6) demultiplexing simultaneously. The red arrows indicate light spots demultiplexed from Bessel beams. CW Laser: continuous wave laser; Mod.: Modulator; EDFA: erbium-doped fiber amplifier; PC: polarization controller; Col.: collimator; SLM: spatial light modulator; BS: beam splitter; Att.: attenuator; OSA: optical spectrum analyzer.

displacements experimentally. As a comparison, we also theoretically calculate the beam wanders of Bessel beams with the same topological charges as demonstrated in the experiments using Eq. (7). The beam wander values $(\langle r_c^2 \rangle^{1/2})$ of the Bessel beams are 27.4 μm, 34.2 μm, 41.4 μm, 47.9 μm, 31.1 μm, 21.3 μm with $\delta T = 23$ K, and 49.7 μm, 85.4 μm, 72.1 μm, 86.5 μm, 67.8 μm, 68.8 μm with $\delta T = 43$ K for J_{-6}, J_{-4}, J_{-2}, J_0, J_2, J_4 and J_6. The Bessel beams shows smaller beam wanders with lower temperature difference and larger topological charge. Turbulence as a random process cannot be simply extracted from the emulation environment. The ensemble average is used to describe the random field. The structure constant C_n^2 is the parameter to indicate the strength of the turbulence, which is typically calculated by experimental data. The experimental results are based on time averages[13,16]. Using the beam wanders values, the structure constant of the turbulent atmosphere are calculated as $C_n^2 = 1.7 \times 10^{-9}\, m^{-2/3}$ with $\delta T = 23$ K and $C_n^2 = 7.2 \times 10^{-9}\, m^{-2/3}$ with $\delta T = 43$ K. We attribute the differences between the theory and the experiment to the statistic of the data in atmospheric turbulence.

Figure 5 shows the BER measurements from the experimental setup as described above. The signal transmitted by the two branched can be considered as unrelated. Therefore signal carried by any Bessel beams from the other branch contribute to crosstalk in the communication system. According to our previous work[5], the adjacent channels contribute the most portion of the crosstalk. The unrelated signals from two paths can satisfy the BER measurement request for multiple channels[22,34]. In our experiment, the SNR is adjusted by an attenuator after the turbulent atmosphere. In principle the beam wander value is irrelevant to power at the fixed turbulence strength[13]. Figure 5(a) shows the BER of the Bessel beams J_2, J_4 and J_{-6} with the temperature difference from room temperature $\delta T = 23$ K. There are BER fluctuations due to beam wanders of Bessel beam in atmospheric turbulence. Since the turbulent atmosphere is random varying during each measurement, the BER values
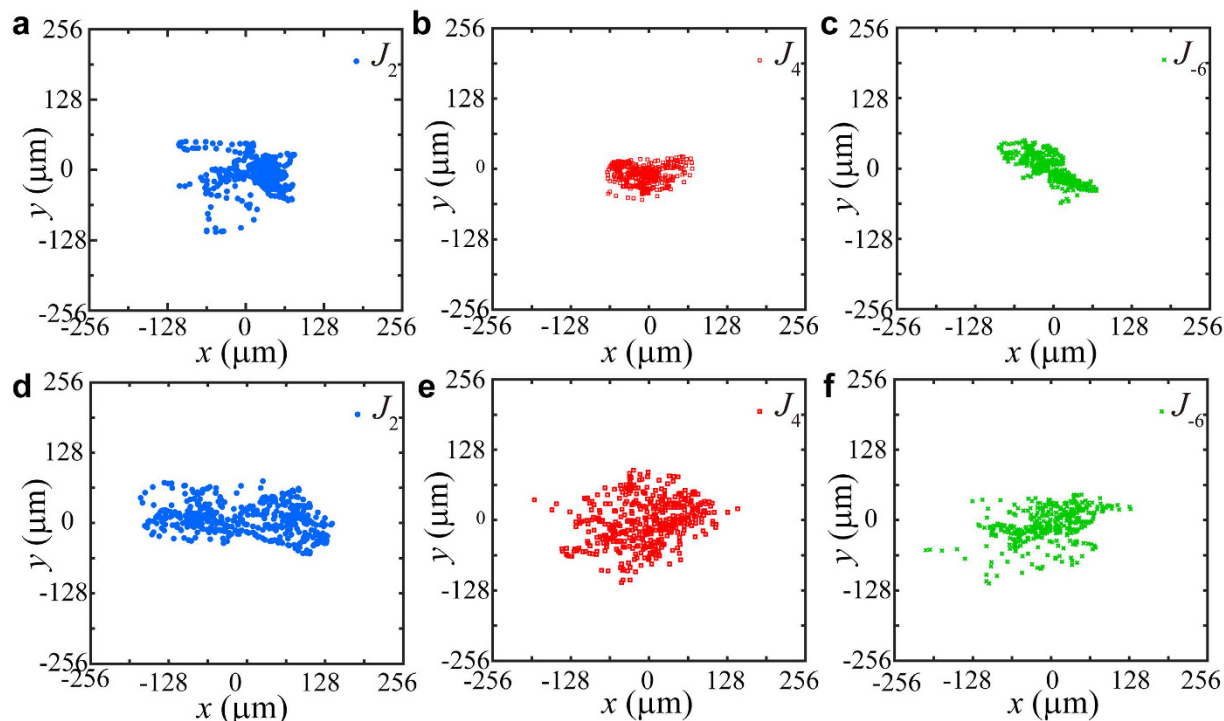
Figure 3. Displacements of high order Bessel beams (J_2, J_4 and J_{-6}) after 1.5 m propagations in turbulent atmosphere at different temperatures. Each dot indicates the central position of the Bessel beams extracted from 488 imaging pictures captured during 30 seconds. The temperature difference from room temperature (T = 300 K) is δT = 23 K in (**a–c**). δT = 43 K in (**d–f**).
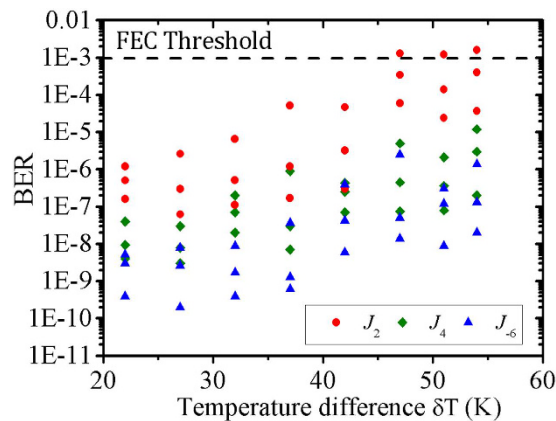

Figure 4. Beam wanders of the Bessel beams (J_2, J_4 and J_{-6}) from theoretical calculation and experimental results at two temperatures difference from room temperature δT = 23 K and δT = 43.

recorded show differences. Especially for the relative low BER value, the random effect is more obvious. With this fixed temperature difference, the Bessel beams with larger topological charges show better communication performance in terms of BER fluctuations and values, which is consistent with the theoretical and experimental results of the beam wanders as shown above. Further increasing the temperature difference to δT = 43 K, the BER measurements still follow the same trend. Although the turbulent atmosphere induce beam wanders and BER fluctuations, all the BERs of the coaxial Bessel beams are still below the forward error correction (FEC) threshold of 1×10^{-3} in this FSO communication link.

Figure 6 shows the BER values varying according to temperature difference δT. The received power is fixed at −12 dBm and the values of the BER are recorded in 30 seconds. In the same condition, the BER shows relative smaller values with larger topological charge. This result is consistent with our theoretical models for the beam wander of the Bessel beams in turbulent atmosphere.
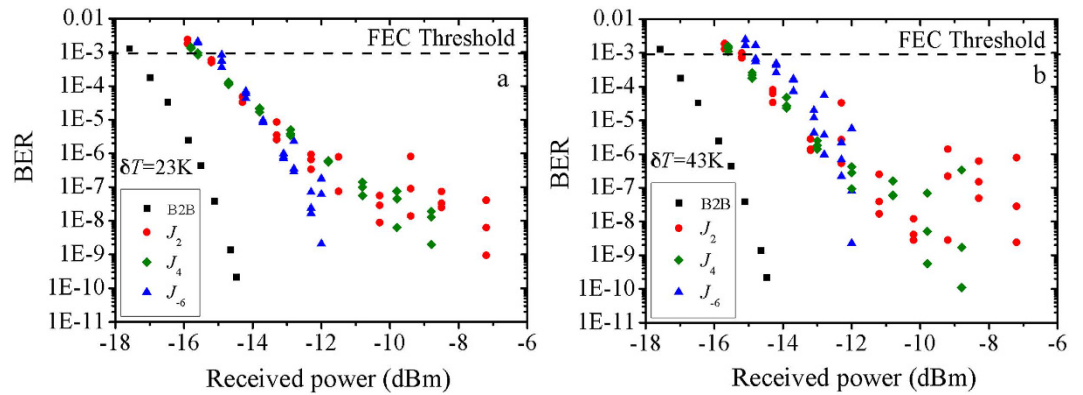
Figure 5. The BER curves of J_2, J_4 and J_{-6} for coaxial Bessel beams $\sum_{n=-3}^{3} J_{2n}$ propagate through turbulent atmosphere demultiplexing in different temperature difference (**a**) $\delta T = 23$ K and (**b**) 43 K.

Figure 6. The BER of J_2, J_4 and J_{-6} with temperature difference δT at fixed received power of -12 dBm.

Discussion

In summary, the beam wanders of the Bessel beams propagating through turbulent atmosphere have been theoretically and experimentally studied. Both experimental data and theoretical calculations show the same trend, that the beams with large topological charge value suffer less effects of turbulent atmosphere. We also multiplex/demultiplex collinear OAM states of Bessel beams by an optical vortex Dammann axicon grating in an FSO link, where the atmospheric turbulence is emulated by a hot plate. The Bessel beams relieved the beam wanders and satisfied the BER criterion for standard OAM multiplexing/demultiplexing in FSO system.

Methods

A standard Gaussian beam carrying high speed signals shines on the phase-only SLM to generate the multiple OAM states of Bessel beams in one branch. The topological charge interval of the Bessel beams is 4. In the other branch multiple Bessel beams carried different signals with the topological charge interval of 4. The two branches multiple Bessel beams are coupled by the beam splitter to generate the multiple OAM states of Bessel beams with the topological charge interval of 2. The perturbation of the turbulent atmosphere is employed by the hot plate. The collinear OAM states of Bessel beams propagating through turbulent atmosphere are simultaneous demultiplexed by the SLM loaded by the optical vortex Dammann axicon grating. The SLM has a resolution of 1920×1080 pixel and the pixel pitch size is 8 μm.

References

1. Uden, R. G. H. V. *et al.* Ultra-high-density spatial division multiplexing with a few-mode multicore fiber. *Nat. Photon.* **8,** 865–870 (2014).
2. Sano, A. *et al.* Ultra-high capacity WDM transmission using spectrally-efficient PDM 16-QAM modulation and C- and extended L-band wideband optical amplification. *J. Lightw. Technol.* **29,** 578–586 (2011).
3. Karl, N. J., McKinney, R. W., Monnai, Y., Mendis, R. & Mittleman, D. M. Frequency-division multiplexing in the terahertz range using a leaky-wave antenna. *Nat. Photon.* **9,** 717–720 (2015).
4. Luo, L. W. *et al.* WDM-compatible mode-division multiplexing on a silicon chip. *Nat. Commun.* **5,** 3069, doi: 10.1038/ncomms4069 (2014).
5. Lei, T. *et al.* Massive individual orbital angular momentum channels for multiplexing enabled by Dammann gratings. *Light Sci. Appl.* **4,** e257, doi: 10.1038/lsa.2015.30 (2015).
6. Wang, J. *et al.* Terabit free-space data transmission employing orbital angular momentum multiplexing. *Nat. Photon.* **6,** 488–496 (2012).

7. Allen, L., Beijersbergen, M. W., Spreeuw, R. J. C. & Woerdman, J. P. Orbital angular momentum of light and the transformation of Lareguer–Gaussian laser modes. *Phys. Rev. A*. **45,** 8185–8189 (1992).
8. Cizmar T. *et al.* Generation and control of multiple Bessel beams for optical micromanipulation. *SPIE* 7038, doi: 10.1117/12.794944 (2008).
9. Davis, J. A., McNamara, D. E., Cottrell, D. M. & Campos, J. Image processing with the radial Hilbert transform: theory and experiments. *Opt. Lett*. **25,** 99–101 (2000).
10. Foo, I. G., Palecios, D. M. & Swartzlander, G. A. Optical vortex coronagraph. *Opt. Lett*. **30,** 3308–3310 (2005).
11. Leach, J., Padgett, M. J., Barnett, S. M., Franke-Arnold, S. & Courtial, J. Measuring the orbital angular momentum of a single photon. *Phys. Rev. Lett*. **88,** 257901 (2002).
12. Andrews, L. C., Phillips, R. L. & Hopen, C. Y. *Laser Beam Scintillation with Applications* (SPIE Press, 2001).
13. Andrews, L. C. & Phillips, R. L. *Laser Beam Propagation through random media* Second edition (SPIE press, 2005).
14. Tatarskii, V. I. *Wave Propagation in a Turbulent Medium* (McGraw-Hill, 1961).
15. Keskin, O., Jolissaint, L. & Bradley, C. Hot-air optical turbulence generator for the testing of adaptive optics systems: principles and characterization. *Appl. Opt*. **45,** 4888–4897 (2006).
16. Anguita, J. A. & Cisternas, J. E. Influence of turbulence strength on temporal correlation of scintillation. *Opt. Lett*. **36,** 1725–1727 (2011).
17. Ren, Y. X. *et al.* Atmospheric turbulence effects on the performance of a free space optical link employing orbital angular momentum multiplexing. *Opt. Lett*. **38,** 4062–4065 (2013).
18. Paterson, C. Atmospheric Turbulence and Orbital Angular Momentum of Single Photons for Optical Communication. *Phys. Rev. Lett*. **94,** 153901 (2005).
19. Anguita, J. A., Neifeld, M. A. & Vasic, B. V. Turbulence-induced channel crosstalk in an orbital angular momentum-multiplexed free-space optical link. *Appl. Opt*. **47,** 2414–2429 (2008).
20. Vallone, G. *et al.* Free-space quantum key distribution by rotation-invariant twisted photons. *Phys. Rev. Lett*. **113,** 060503 (2014).
21. Krenn, M. *et al.* Communication with spatially modulated light through turbulent air across Vienna. *New J. Phys*. **16,** 113028 (2014).
22. Ren, Y. X. *et al.* Experimental characterization of a 400 Gbit/s orbital angular momentum multiplexed free-space optical link over 120-meters. *Opt. Lett*. **41,** 622–625 (2016).
23. Ahmed, N. *et al.* Experimental Demonstration of Obstruction-Tolerant Free-Space Transmission of Two 50-Gbaud QPSK Data Channels using Bessel Beams carrying Orbital Angular Momentum. The European Conference on Optical Communication (ECOC). 10.1109/ECOC.2014.6964157 (2014).
24. Lukin, I. P. Variance of fluctuations of the orbital angular momentum of Bessel beam in turbulent atmosphere. *SPIE* 8696, doi: 10.1117/12.2008730 (2012).
25. Zhu, K. C., Li, S. X., Tang, Y., Yu, Y. & Tang, H. Q. Study on the propagation parameters of Bessel–Gaussian beams carrying optical vortices through atmospheric turbulence. *J. Opt. Soc. Am. A*. **29,** 251–257 (2012).
26. Lukin, I. P. Random displacement of the Bessel–Gaussian beam in turbulent atmosphere. *SPIE* 9292, doi: 10.1117/12.2074472 (2014).
27. Ahmed, N. *et al.* Mode-Division-Multiplexing of Multiple Bessel-Gaussian Beams Carrying Orbital-Angular-Momentum for Obstruction-Tolerant Free-Space Optical and Millimetre-Wave Communication Links. *Sci. Rep*. **6,** 22082, doi: 10.1038/srep22082 (2016).
28. Xu, Z. D., Zhou, J. Y., Gui, C. C. & Wang, J. Bessel Beam Multiplexing for Free-Space Optical Communications Assisted by 6 × 6 MIMO Equalization, *Asia Commun. Photon. Conference. OSA*, ATh3A 110 (2014).
29. Zhu, L. & Wang, J. Demonstration of obstruction-free data-carrying N-fold Bessel modes multicasting from a single Gaussian mode. *Opt. Lett*. **40,** 5463–5466 (2015).
30. Davis, J. A., Guertin, J. & Cottrell, D. M. Diffraction-free beams generated with programmable spatial light modulators. *Appl. Opt*. **32,** 6368–6370 (1993).
31. Arrizón, V., Ruiz, U., Aguirre-Olivas, D., Sánchez-de-la-Llave, D. & Ostrovsky, A. S. Comparing efficiency and accuracy of the kinoform and the helical axicon as Bessel–Gauss beam generators. *J. Opt. Soc. Am. A*. **31,** 487–492 (2014).
32. Yuan, Y. S. *et al.* Parallel Detection of OAM States Carried by Coaxial Bessel Beams. *IEEE Photon. Technol. Lett*. **28,** 315–318 (2016).
33. García-Martínez, P. *et al.* Generation of Bessel beam arrays through Dammann gratings. *Appl. Opt*. **51,** 1375–1381 (2012).
34. Gao, S. C. *et al.* OAM-labeled free-space optical flow routing. *Opt. Express*. **24,** 21642–21651 (2016).

Acknowledgements

Author Contributions

Y.Y., T.L. and X.Y. conceived the concept and experiment. Y.Y., Y.L. and S.G. accomplished the experiment. Y.Y. and Z.X. deal with the experimental data. Y.Y. and T.L. contributed to writing the paper. Z.L. and X.Y. monitor the program.

Additional Information

Competing financial interests: The authors declare no competing financial interests.

How to cite this article: Yuan, Y. *et al.* Beam wander relieved orbital angular momentum communication in turbulent atmosphere using Bessel beams. *Sci. Rep.* **7,** 42276; doi: 10.1038/srep42276 (2017).

Publisher's note: Springer Nature remains neutral with regard to jurisdictional claims in published maps and institutional affiliations.